Agronomy Research **14**(S1), 1088–1098, 2016

Electrical field based detection of fruits and vegetables for robotized horticulture

V. Osadcuks* and A. Pecka

Latvia University of Agriculture, Faculty of Engineering, Department of Energetics, Cakstes blvd. 5, LV-3001 Jelgava, Latvia; *Correspondence: vtl@tvnet.lv

Abstract. In this research authors study possibilities of using transmitting-type electric field based sensors for recognition of fruits and vegetables. The main idea is to detect distortions of electrical field between electrodes of sensors by measuring capacitance changes for these electrodes. Electrical field is strongly affected by relative permittivity of medium, which is several times larger for fruits and vegetables consisting mainly of water than for surrounding air, leaves and other low-mass non-conductive objects. This could help to develop electrical field sensing device with number of electrodes for detection of fruits or vegetables and determining their position thus serving as additional sensor in multi sensor system with optical camera or as stand alone device. The research covers both theoretical aspect of proposed approach and experimental evaluation of prototype device based on mixed signal controller MGC3130 originally intended for electrical field based gesture sensing periphery for consumer electronics. Main results show that in worst condition when an electrode is fully covered with a physical model of leaf 43% of signal value in comparison to sensor output without obstacle is still usable. Thus this type of sensors potentially can be an integral part of complex fruit or vegetable recognition system in robotized horticulture applications.

Key words: electrical field, sensor, horticulture, fruit and vegetable recognition.

INTRODUCTION

Reliable, fast and energy-efficient recognition and determination of spatial position and orientation of fruits and vegetables is one of key tasks for agricultural robots to be technically and economically efficient in precision application of plant protection products and harvesting tasks. In majority of experimental agricultural robots prototypes and solutions this task is accomplished by using computer vision systems in various spectral ranges. Main drawbacks of this approach are computational power and recognition speed tradeoffs, sensitivity to changes in ambient lighting, necessity of readjustment for various species and even degrees of ripeness, difficulties to recognize objects of interest in heavy foliage and affection by atmospheric conditions (for, rain, dust etc.) (Cohen et al., 2011) as well as difficulties to select proper recognition algorithm for these changing conditions (Fernández et al., 2014).

Capacitive sensing is used very widely nowadays. Beginning from automation applications in industrial environment (Taghinezhad et al., 2012) to power saving using human body detection in appliances and smart homes and consumer electronics (Villiers, 2012) with focus on various types of HMI.

Mainly there are three modes of capacitive sensing: loading mode, shunt mode and transmit mode, in this study the latter one is used, which gives the longest sensing range. Transmit mode uses a transmitting electrode that is coupled to a conductive object. The properties of an alternating electric field generated with respect to a receiving electrode will therefore depend on the distance of this body, thus extending the achievable range (Smith, 1996; Brauna et al., 2015).

This type of sensing technology could hypothetically substitute or supplement computer vision based sensors in situations where they fail to recognize fruit or vegetable under canopy, in adverse conditions for optical systems or when processing power and optical equipment necessary for successful completion of the task makes them economically and practically ineffective. Electrical field is strongly affected by relative permittivity of medium, which is several times larger for fruits and vegetables consisting mainly of water than for surrounding air, leaves and other low-mass non-conductive objects. This could help to develop electrical field sensing device with number of electrodes for detection of fruits or vegetables and determining their position.

The aim of the study is to find if it is practically possible to use transmitter-receiver type electrical field based sensor for detection and position measurement of fruits and vegetables under cover by surrounding canopy.

In this study authors use integrated mixed signal chip manufactured by Microchip Inc. MGC3130 which uses manufacturers proprietary GestIC technology to give the proof of concept for near E-field sensing of vegetables and fruits in robotized horticulture applications. The experiments consisted of positioning a detectable object over the sensor with and without obstacles and measuring field strength. Positioning was automated using V-plotter type CNC machine.

MATERIALS AND METHODS

Equivalent circuit for MGC3130 chip based E-field sensing electrode system is given in Fig. 1. It consists of transmitting and receiving electrodes E_{Tx}, E_{Rx}, ground plane, capacitances between electrodes and ground plane, transmitting driver and receiving buffer.

The sensing system operates by measuring voltage on capacitance voltage divider formed by C_{RxTx}, C_L as upper side and C_{RxG}, C_{Obj}, C_{Buf} as lower side. Transmitter provides square wave signal U_{Tx} at frequencies 44–115 kHz (can be changed depending on external noise conditions) to transmitting electrode, and after division it is measured at receiver as U_{Rx}. Magnitude of signal can be expressed according to voltage divider equation (1) (Microchip Inc., 2013a).

$$U_{Rx} = \frac{U_{Tx}}{1 + \frac{C_{RxG} + C_{Buf} + C_{Obj}}{C_{RxTx} + C_L}}. \quad (1)$$

When there is no object in vicinity C_{Obj} approaches to zero. Receiver should be capable to detect voltage changes on divider when object distorts electrical field and changes C_{Obj}. Because input buffer load is too high to measure U_{Rx} voltage directly without specific parameterisation procedures, receiver simply measures the difference

of signal ΔS when $C_{Obj} = 0$ and when it changes assuming that C_{Obj} is much smaller than electrode mutual and ground capacitances (Microchip Inc., 2013a):

$$\Delta S = U_{Rx}\left(C_{Obj} = 0\right) - U_{Rx}\left(C_{Obj} > 0\right) = \\ = \frac{U_{Tx} C_{Obj}}{C_{RxTx} + C_L + 2\left(C_{RxG} + C_{Buf}\right) + \frac{\left(C_{RxG} + C_{Buf}\right)^2}{C_{RxTx} + C_L}}. \quad (2)$$

Signal value when $C_{Obj} = 0$ is obtained by reading and storing U_{Rx} when there is no object in vicinity, thus calibration is performed.

End signal after amplification and preprocessing which is carried out by MGC3130 built-in DSP is defined as signal deviation S_D, which relates to gain of 10 times, measurement voltage range of 3 V and half of ADC resolution and is given as 16 bit signed dimensionless integer value (Microchip Inc., 2013a):

$$S_D = 10 \cdot \frac{2^{15}}{3\text{V}} \Delta S. \quad (3)$$

This value is used as signal relative strength in measurements of object's approach to the sensor.

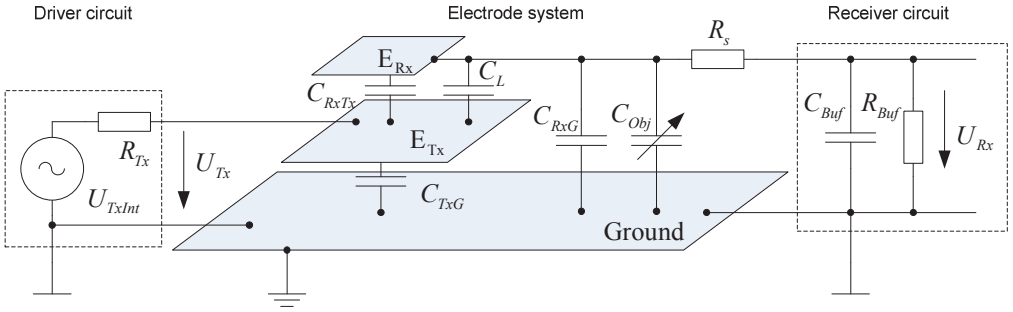

Figure 1. Equivalent circuit of single electrode and MGC3130 output driver and inpud buffer: E_{Rx} – receiver electrode; E_{Tx} – transmitter electrode; U_{TxInt} – internal transmitter signal; U_{Tx} – signal on driver's output pin; U_{Rx} – received signal; R_{Tx} – driver source resistance; R_{Buf} – resistance of MGC3130 input buffer; R_s – series resistance between E_{Rx} and MGC3130 input pin, can be increased for high frequency noise suppression (1 kΩ on evaluation board); C_{TxG} – capacitance from transmitter to ground; C_{RxTx} – capacitance between E_{Tx} and E_{Rx} electrodes; C_L – receivers interconnection wire's capacitance to transmitter electrode; C_{RxG} – capacitance from receiver to ground; C_{Obj} – capacitance between sensed object and ground; C_{Buf} – capacitance of MGC3130 input buffer (Microchip Inc., 2013a).

In experiments MGC3130 Sabrewing evaluation board was used, which has 5 electrodes, E-field sensing chip and USB interface for connection to PC (Microchip Inc., 2013b), physical configuration and dimensions of electrodes are given in Fig. 2.

The electrode system is built in 4-layer 1.5 mm receiving electrode on top of the stacks, transmitting electrode and interconnection wires for receivers at 3rd layer and ground plane at the bottom layer. Transmitting electrode is formed as mesh and covers

all board's sensing area. Receiving electrodes at the edges of board are made as solid copper, but large centre electrode is formed as a mesh in order to make signal level approximately equal to those on edges of sensor board. Interconnection wires between receivers are built in between transmitter wiring in 3rd layer thus improving noise immunity.

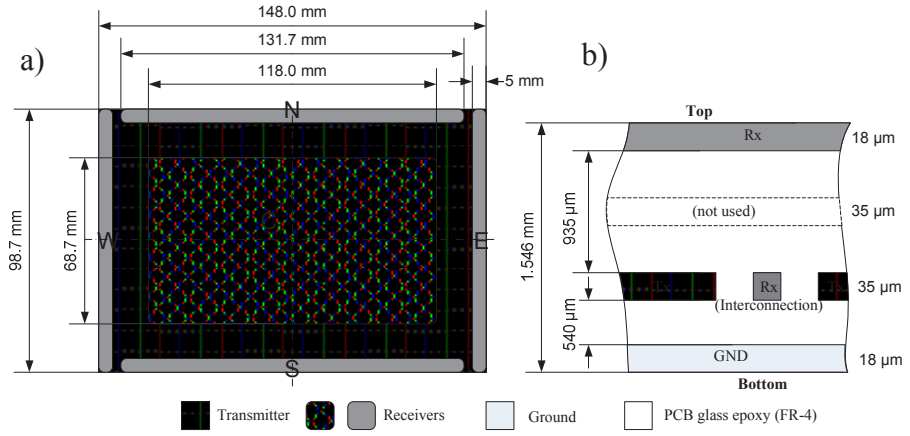

Figure 2. Physical configuration and dimensions of electrodes in evaluation board: a – top view (ground plane not seen); b – cross section of PCB layers (Microchip Inc., 2013b).

Experimental setup (Fig. 3) consists of sensor (GestIC evaluation board), CNC positioning mechanism and controlling computer with two interfaces for sensor and motor control running ungrounded on batteries. Grounded shielding plate is placed under the sensor board. Arrangement of the setup was chosen to minimise unwanted electrical fields and charge build-ups on sensed object.

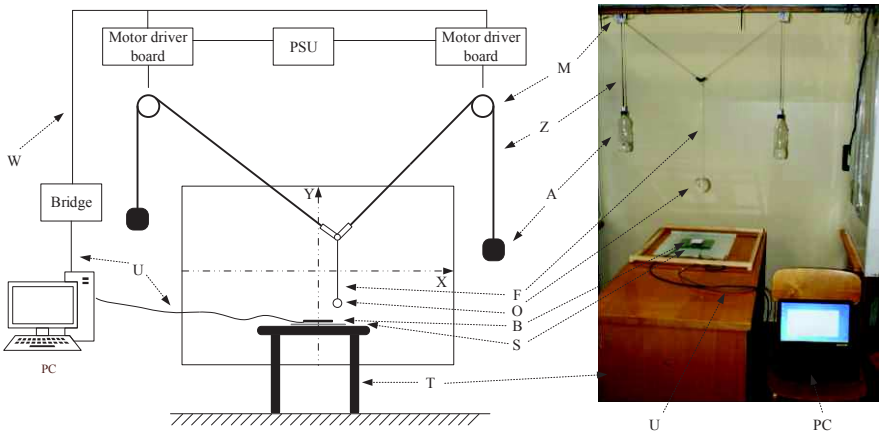

Figure 3. Experimental setup: A – balance weight; B – evaluation board; F – fishing lines; M – steper motor; O – object to sense; S – ground shield; T – table; U – USB cable; W – UART cable; Z – toothed belts.

Plastic sphere with 80 mm external diameter filled with mains water was used as a detectable object. Total mass of plastic – 32 g, water – 230 g. Positioning precision for all experiments was 0.5 mm.

Three types of experiments with approaching object were performed (see Fig. 4). The detectable object was moved near to and away from the sensor by 0.5 mm for vertical and 0.2 mm steps for horizontal movement every 100 ms. Step size and time was chosen to minimise unwanted oscillations of sphere due to its inertia. Signal deviation signal for all electrodes was measured before each step. MGC3130 chip can perform and report up to 200 measurements per second thus experimental data is fully static.

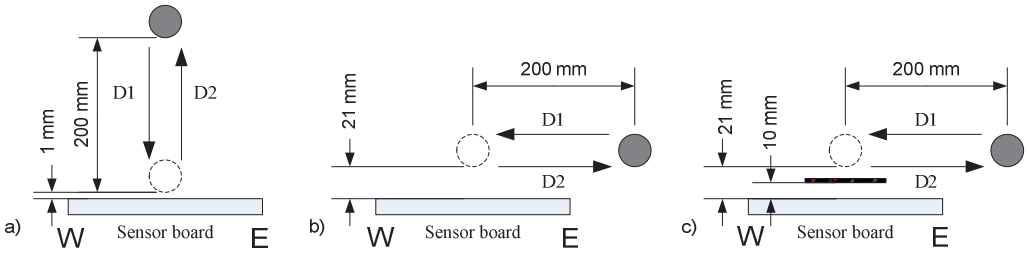

Figure 4. Types of experiments: a – object approaching from top; b – object approaching from side; c – object approaching from side with obstacle between detectable object and sensor.

Experiment ‘a’ was intended to evaluate signal produced by approaching object at various distances. Starting position for object was 201 mm above sensor i.e. distance between sensor and bottom of the sphere. Then sphere was moved down (direction D1) down to 1 mm above sensor then back up to the same position (direction D2) thus performing one test run.

At the same time during the experiment type ‘a’ influence of sensing frequency was evaluated. As external noise was minimum during experiments (see the Results section), significant differences in sensing distances for various operating frequencies were not observed. Therefore all available frequencies (44 kHz, 67 kHz, 88 kHz, 103 kHz and 115 kHz) were allowed for MGC3130 to automatically select to minimize existing external noise effect during rest of the experiments.

Experiments ‘b’ and ‘c’ were performed at constant distance between sensor and object – 21 mm to compare performance of object sensing with and without obstacles.

Obstacle in experiment ‘c’ was placed to demonstrate possible system performance in real life situation when detectable object (fruit or vegetable) is covered by plant’s canopy. To model obstacle – plant’s leave with some content of water and non-transparent, standard 80 g m^{-2} office paper sheet was saturated with mains water and placed in hermetic plastic bag to prevent evaporation. Two sizes of sheets were used: 60 x 60 mm and 120 x 70 mm, sheets were placed at 10 mm distance at the centre of the sensor board. Sizes were selected to cover Centre electrode partially and fully and to approximately reflect typical dimensions of plant leaves. Fishing lines were used to position paper sheets to minimise influence on sensor.

In experiment ‘a’ for signal strength measurement 12 test runs were performed; and one test run for each measurement frequency (5 in total). For each experiment ‘b’ and ‘c’ 4 test runs were made.

Calibration of signal (measurement of ambient signal without test object in vicinity) was carried out before each test run in direction D1. With exceptions for experiment ‘c’ where calibration was done without obstacle prior to all test runs to avoid calibrating on obstacle’s distortions in E-field.

RESULTS AND DISCUSSION

Results of the experiments as S_D signals as functions of distance from detectable object to sensor are presented in Figs 5–12. Detectable object movement from and to sensor is shown in separate graphs and the object’s closest point to the sensor (1 mm above sensor for experiment ‘a’ and 21 mm above in the centre position of sensor for experiments ‘b’ and ‘c’) is shown on both graphs.

For vertical object approach (Fig. 5) it can be seen that S_D is increasing exponentially and object’s presence can be detected already at distance of 90 mm where it rises over noise RMS level 5.6 without object in vicinity (dashed line).

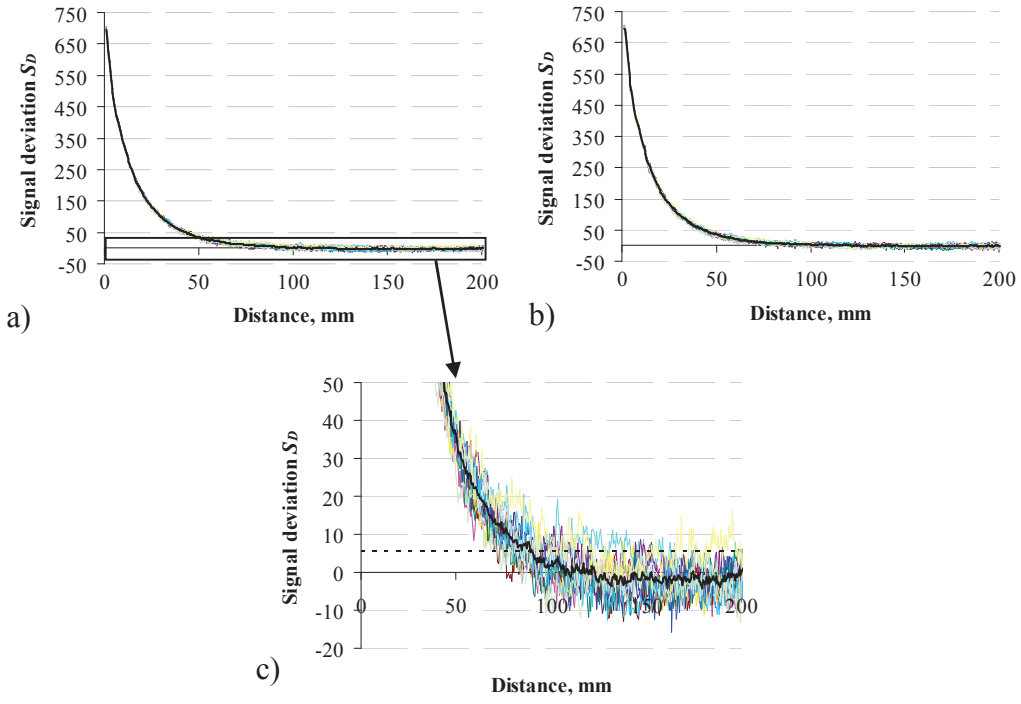

Figure 5. Results of experiment ‘a’ for centre electrode, 12 runs and average line in bold: a – direction D1 (moving to sensor); b – direction D2 (moving away from sensor); c – zoom of detection signal area.

Electrodes on the edges of the sensor were also affected, which is shown on distance's logarithmic scale for better visibility in Fig. 6. As the object approaches S_D for edge electrodes at first increased then started to fall below noise level, the explanation could be that object with larger than air permittivity attracted majority of electrical field lines. Thus field strength over edges of the sensors and consequently received signal U_{Rx} felt.

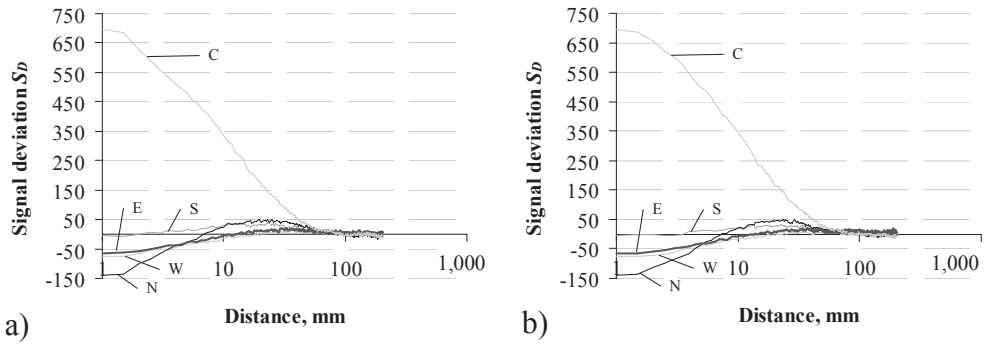

Figure 6. Results of a single run in experiment 'a' for all electrodes (in logartihmic scale): a – direction D1; b – direction D2.

Altogh effect of signal frequency was insignificant (Fig. 7) a trend could be observed that signal strength slightly increases proportionally to frequency. This can be better seen at close distances, and frequency has no effect on noise level when there is no object nearby.

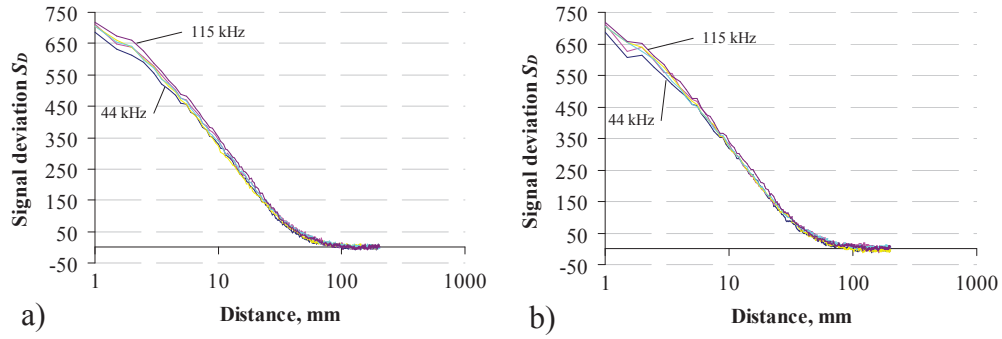

Figure 7. Effect of transmitting signal frequency for experiment 'a' (in logartihmic scale): a – direction D1; b – direction D2.

Experiment ‘b’ (see Fig. 8 for average values of center electrode and 9 for a single run and all electrodes) demonstrates performance of sensor in a fixed height over sensor and approachment of the object form electrode E side.

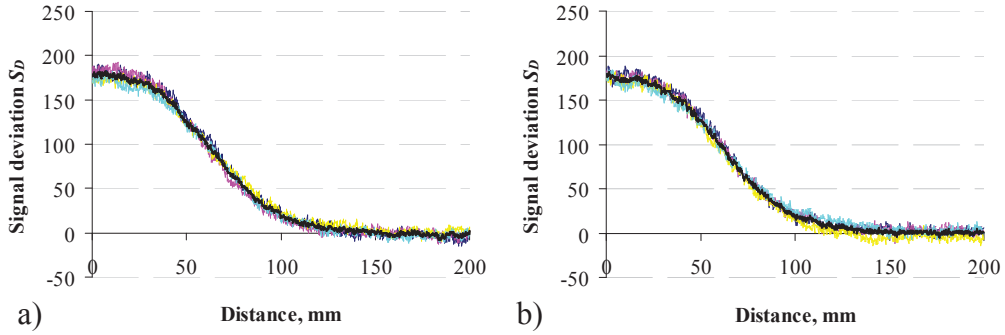

Figure 8. Results of experiment ‘b’, 4 runs and average line in bold: a – direction D1; b – direction D2.

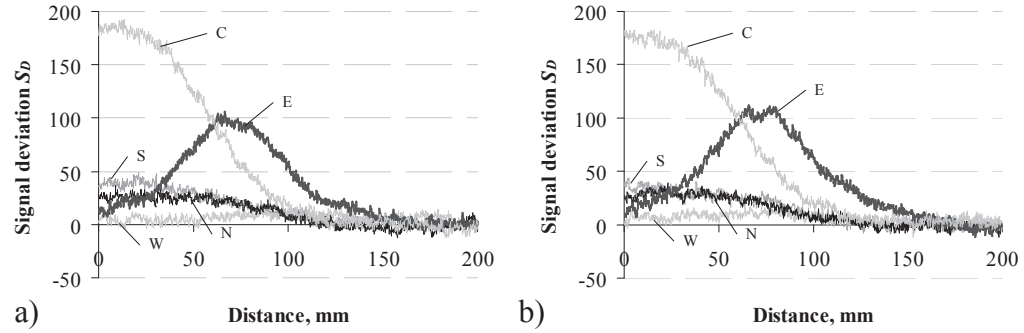

Figure 9. Results of a single run in experiment ‘b’ for all electrodes: a – direction D1; b – direction D2.

Graph for all elctrodes shows how signals are changing when the detectable object passes over. Sequential change in signal levels allows to determine position of the masss centre of the object. In original application of the sensor board this is used to detect hand gestures and determine the position of hand relative to sensor, the same approach potentially could also be used for determination of fruit’s or vegetable’s position. This data is used to compare how sensor will react if it is covered by obstacle in experiment ‘c’ (Figs 10–12).

When obstacle was placed 10 mm above sensor, S_D increased proportionally to size of the obstacle. Similarly as it was to spherical object signal of Centre electrode in comparison to ambient noise increased, but on the edges – decreased, thus signal with no object is grater than 0 (Figs 10, 11). Difference of S_D maximum level when detectable object reached central position of sensor and ambient level decreased with increase of obstacle's area – 180 without obstacle, 162 for 60 x 60 mm obstacle and 77 for 120 x 70 mm obstacle. Thus in the worst condition when the central electrode was fully covered with a "leaf" we got 43% of usable signal value of S_D without obstacle.

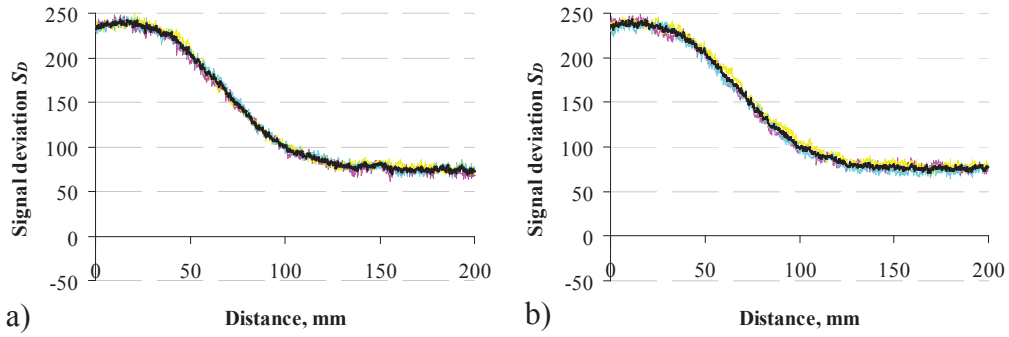

Figure 10. Results of experiment 'c' with 60 x 60 mm obstacle at the centre of electrode C, 4 runs and average line in bold: a – direction D1; b – direction D2.

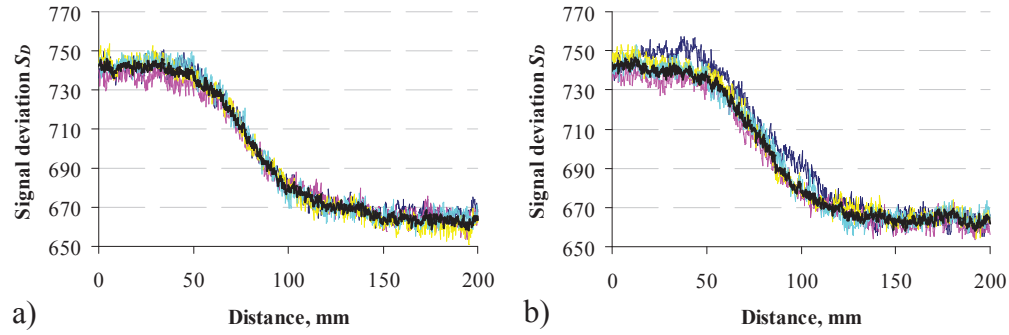

Figure 11. Results of experiment 'c' with 120 x 70 mm obstacle at the central electrode, 4 runs and average line in bold: a – direction D1; b – direction D2.

Fig. 12 shows development of S_D signal on East and Centre electrodes where detectable object passed over with obstacle between it and the sensor. The rest of electrodes are not shown, because their S_D values were out of range in comparison to Centre and East electrodes. Although change between minimum and maximum levels decreases with size of the obstacle (note the scales of Y axis in figures) it is still possible to determine transitions of signal level on both electrodes and thus to determine position of detectable object.

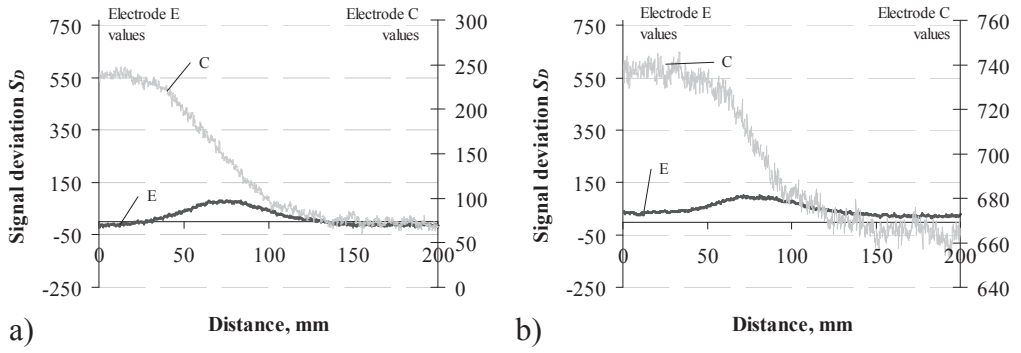

Figure 12. Signal strength on C and E electrodes for a single test in experiment 'c': a – for 60x60 mm obstacle; b – for 120 x 70 mm obstacle.

It is clear that in real life situations in horticulture and other biological applications for robotized automation to be cost-effective and reliable it is necessary to combine various types of sensors (Zujevs et al., 2015).

Object detection when direct visual contact with object of interest is not needed allows to apply the proposed electrical field based sensing as a supplement of computational vision in such use cases as:

- pre-operation – identifying areas for subsequent precise vision-based examination of vegetables to decrease necessary computing power for image processing and increasing recognition speed;
- post-operation – increasing recognition system reliability by distinguishing of vegetables or fruits between other objects if partially covered or in adverse optical conditions such as dust, direct or shadow-casting illumination, humidity etc.;
- fine adjustment of manipulator position for plant treatment or harvesting.

In order to evaluate the possibilities of application of E-field based sensing in these areas in further research it is necessary to build simulation model of the sensor, design electrode layout and finding optimum transmitting signal parameters, to develop the prototype and perform experimental testing in real-life conditions.

CONCLUSIONS

1. The main idea of the study was to show that it is practically possible to use transmitter-receiver type electrical field based sensor for detection and position measurement of fruits and vegetables under cover by surrounding canopy.

2. Development board based on Microchip GestIC technology and MGC3130 mixed signal controller was used in this study as a sensor. The board is originally intended as a gesture detection and recognition device for data input in PCs.

3. Experiments show that despite of decrease in signal to noise ratio when detection electrode is fully covered, position of detectable object is still determinable. In worst condition when an electrode is fully covered with a physical model of leaf 43% of signal value in comparison to sensor output without obstacle is still usable.

4. Changes in transmitting signal frequency in laboratory conditions had no significant results, but there was a trend in increase of detectable signal strength with increase of frequency.

5. Electrical field based sensors in essence have no limitations distinctive for optical computer vision systems as these detect only object's mass with different permittivity, but also doubtless have own drawbacks – they need frequent calibration without any objects in vicinity as electrical charges my build up on them during operation, they cannot be used for fine quality control and for recognition of relatively small objects. Thus this type of sensors potentially can be an integral part of complex fruit or vegetable recognition system in robotized horticulture applications.

REFERENCES

Villiers, G. 2012. How capacitive sensing can reduce standby power in household appliances. Embedded. [online][15.01.2016.] http://www.embedded.com/print/4395685.

Taghinezhad, J., Alimardani, R. & Jafari, A. 2012. Development of a Capacitive Sensing Device for Prediction of Water Content inSugarcanes Stalks. *International Journal of Advanced Science and Technology* **44**, 61–68.

Zujevs, A., Osadcuks, V. & Ahrendt, P. 2015. Trends in Robotic Sensor Technologies for Fruit Harvesting: 2010–2015. *Procedia Computer Science* **77**, 227–233.

Brauna, A., Wicherta, R., Kuijpera, A. & Fellner, D.W. 2015. Capacitive proximity sensing in smart environments. *Journal of Ambient Intelligence and Smart Environments* **7**(4), 483–510.

Microchip Inc. 2013. Application note DS40001716A, 82 p.

Microchip Inc. 2013. Application note DS41685A, 34 p.

Smith, J.R. 1996. Field mice: Extracting hand geometry from electric field measurements. *IBM Syst. J.* **35**(3.4), pp. 587–608.

Cohen, O., Linker, R. & Naor, A. 2011. *Estimation of the Number of Apples in Color Images Recorded in Orchards. Computer and Computing Technologies in Agriculture IV*. **344**, 630–642.

Fernández, R., Salinas, C., Montes, H. & Sarria, J. 2014. Multisensory System for Fruit Harvesting Robots. Experimental Testing in Natural Scenarios and with Different Kinds of Crops. *Sensors* **14**(12), 23885–23904.